Journal of Energy Storage 153 (2026) 120994

Contents lists available at ScienceDirect

Journal of Energy Storage

journal homepage: www.elsevier.com/locate/est

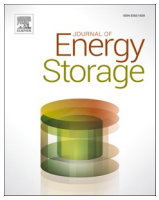

Research papers

Influence of CO_2 in the Li-ion battery-production atmosphere on the sorption kinetics of $Li[Ni_{0.6}Co_{0.2}Mn_{0.2}]O_2$ and its effect on cell performance

Thilo Heckmann [a,*], Maximilian Lechner [b], Philipp Barbig [a], Xiangling Gui [b], Lukas Madlindl [a], Philip Scharfer [a], Rüdiger Daub [b,c], Wilhelm Schabel [a]

[a] Karlsruhe Institute of Technology (KIT), Thin Film Technology (TFT), Karlsruhe, 76131, Germany
[b] Institute for Machine Tools and Industrial Management, Technical University of Munich (TUM), Boltzmannstraße 15, 85748, Garching, Germany
[c] Fraunhofer Institute for Casting, Composite and Processing Technology (IGCV), Am Technologiezentrum 10, 86159, Augsburg, Germany

ARTICLE INFO

Keywords:
Lithium-ion batteries
NMC cathodes
Moisture management
Sorption
Degradation

ABSTRACT

Water inside a Li-ion battery (LiB) can be detrimental to its performance and even degrade cathode active materials (CAM) in combination with CO_2 during production. This degradation may originate from sorption of water and CO_2 in CAM. Moisture management aims to control this sorption process, minimize degradation, and reduce water carried into the cell during production. Controlling these sorption processes requires understanding the kinetics that restrict the mass uptake of water and CO_2 in CAM. This manuscript provides time-resolved sorption data for $Li[Ni_{0.6}Co_{0.2}Mn_{0.2}]O_2$ (NMC-622) and $Li[Ni_{0.8}Co_{0.1}Mn_{0.1}]O_2$ (NMC-811) cathodes as electrodes and NMC-622 CAM as powder in various humid atmospheres. The exposed material was processed to full coin cells and electrochemically tested. The sorption behavior of cathodes in air at 72%-RH is restricted by kinetics depending on material chemistry. Experiments showed the difference in sorption behavior of NMC-622 in humid atmospheres with and without CO_2. The exposure of CAM to humid atmospheres with various CO_2 concentrations showed that cell performance decreases with increasing CO_2 concentration in the atmosphere – linking a defined mass uptake of NMC-622 from water and CO_2 to a capacity loss. The overall mass uptake detected at industrially relevant conditions in NMC-622 in four days is ~250 wt-ppm, which has little but noticeable effect on cell performance.

1. Introduction

The atmosphere in the production facility of lithium-ion batteries (LiB) influences the cell performance, because water and carbon dioxide (CO_2) interact with the components of a LiB cell [1–6]. A LiB-cell production process consists of the electrode production as well as cell assembly and cell conditioning [1]. Depending on the process configuration the active material of the cell may be exposed to the production atmosphere until the cell is filled with electrolyte and sealed. Ample publications discuss the negative effect of water (either absorbed from production atmosphere or as solvent residue from water-based coating processes) on the cells performance [7–10]. It has also been shown that cathode active materials (CAM) chemically bind water and CO_2 which degrades the material and affects cell performance as well [11,12]. Mitigating the effects of water and CO_2 is essential for producing LiBs efficiently while conserving energy and material resources [11–13]. Understanding the interaction between the CAM and water and CO_2 if the CAM is exposed to humid atmospheres is the first step to mitigate the effects of water and CO_2.

The motivation of this study is to understand the interaction between CAM and water and CO_2, which chemically degrade the CAM through chemisorption. The effect of chemical degradation has been shown by many studies. Schuer et al. exposed the CAM $Li[Ni_{0.8}Co_{0.1}Mn_{0.1}]O_2$ (NMC-811) to humid air and demonstrated a change in the surface morphology along with a negative effect on the cell performance [14]. Sicklinger et al. and Jung et al. provided detailed insights into the effect of the chemical degradation on cell performance as well as the underlying chemical reactions [15,16]. Chen et al. varied exposure times to humid air and showed the effects of the resulting degradation on the CAM [17]. These studies show the importance of controlling CAM degradation.

The described chemical interaction takes place throughout the production chain of the electrodes during which the CAM is exposed to air. The formation of hydroxy species is the first step during which metal, e.

* Corresponding author.
E-mail address: thilo.heckmann@kit.edu (T. Heckmann).

https://doi.org/10.1016/j.est.2026.120994
Received 24 July 2025; Received in revised form 29 December 2025; Accepted 5 February 2026
Available online 10 February 2026
2352-152X/© 2026 The Authors. Published by Elsevier Ltd. This is an open access article under the CC BY license (http://creativecommons.org/licenses/by/4.0/).

g., lithium from the CAM, reacts with water [18]. Subsequently, these hydroxy species may react to carbonates with the CO_2 from ambient air [19]. Zou et al. found a passivating layer of LiOH on the surface of Li$[Ni_{0.3}Co_{0.3}Mn_{0.3}]O_2$ (NMC-111), Li$[Ni_{0.6}Co_{0.2}Mn_{0.2}]O_2$ (NMC-622), and NMC-811, whereby the layer thickness grows with increasing nickel content [18]. Furthermore, water uptake in the form of hydrates could also occur in the presence of hydroxy species [20]. Sicklinger et al. investigated the reversibility of these species and showed which molecules desorb from deteriorated CAM as a function of temperature [15]. These studies fundamentally investigate the possible mechanisms of CAM degradation during the production of electrodes.

This work provides insights into the sorption of water and CO2 in NMC-622 cathodes and powder at defined atmospheres. Experiments were conducted with air and nitrogen and CO_2 at defined dew-point temperatures. An electrochemical analysis assesses the severity of the exposure after a defined mass-uptake of CO_2 and water. The novelty of this study is experimental data of time-resolved sorption kinetics of CAM as raw material in atmospheres with varying CO_2 concentrations associated to cell performance data. Additionally, this experimental data is evaluated regarding limiting mass-transport resistances. This study aims to incorporate the present fundamental knowledge to interpret the experiments from a process engineering perspective.

2. Materials and methods

The cathodes for sorption experiments in the desiccator were produced according to Huttner et al. and Heck et al. [21,22]. The anodes for the sorption experiments in the desiccator were prepared according to Kumberg et al. [23]. The CAM NMC 622 from BASF was used as received and transferred into sample vials in a glove box. Electrode production for cell testing is indicated below.

Setup 1: A super-saturated salt solution, made from Strontium Chloride Hexahydrate (Carl Roth GmbH & Co. KG, Germany) and distilled water, adjusted the relative humidity inside the desiccator. The sample vials were placed on a perforated bottom inside the desiccator. The perforated bottom allows gas exchange inside the desiccator. With increasing time intervals, the sample vials, filled with cathode electrodes, were weighed. This routine consisted of sealing the vials via ground-joint lids and transferring them to a high-resolution balance. The sampling of the cathode electrodes was performed in triplets and sampling of the anode electrode in doublets.

Setup 2: The sorption apparatus, schematically shown in Fig. 1, measures time-resolved sorption curves and isotherms. This setup has been used in multiple studies to assess sorption behavior of battery materials and others [2,24–27]. A mass change of 10^{-5} g in the sample can be logged over time. The atmosphere in the measurement cell is adjusted via a mixture of water-saturated and pure gases [25,28]. This setup was used to probe CAM as raw material.

Exposition of CAM in addition to Setup 2: Additional CAM as raw material (for cell testing) was exposed to the same gas stream that perfuses through the measurement cell. The CAM was evenly distributed in a petri dish placed under a nozzle in the desiccator, cf. Fig. 1. The gas outlet of the desiccator via a receiver adapter was placed in the same ground socket in the desiccator, to assure a uniform gas flow field inside the desiccator. After exposure, the CAM as raw material was transferred into a glovebox, processed to cathodes, and prepared for cell testing.

To investigate the impact of the CAM exposition on electrochemical performance, coin full-cells were built. Table 1 provides the composition and target properties of the electrodes for the coin cells.

2.1. Slurry mixing

To prepare the anode slurry, sodium carboxymethyl cellulose (CMC) (Merck, Germany) and distilled water were mixed at 2000 rpm for 40 min in a disperser (FM10, VMA-Getzmann, Germany). Using a rotary revolution mixer (Speedmixer DAC 1100.2 VAC-P, Hauschild, Germany), Graphite (SMG-A5, Showa Denko, Japan) and a conductive additive (Super C65, Imerys, France) were dry mixed at 1400 rpm for 1

Table 1
Composition and target properties of the electrodes for the coin cells.

		Anode		Cathode	
		Material	Fraction	Material	Fraction
Composition	Active material	Graphite	94 wt%	NMC-622	96 wt%
	Binder 1	CMC	2 wt%	PVDF	2 wt%
	Binder 2	SBR	3 wt%	–	–
	Conductive additive	C65	1 wt%	C65	2 wt%
	Areal capacity	3.2 mAh cm^{-2}		2.9 mAh cm^{-2}	
	Porosity	30%		30%	
Properties	Electrode diameter	15 mm		14 mm	
	Current collector	Copper / 12 µm		Aluminum / 15 µm	

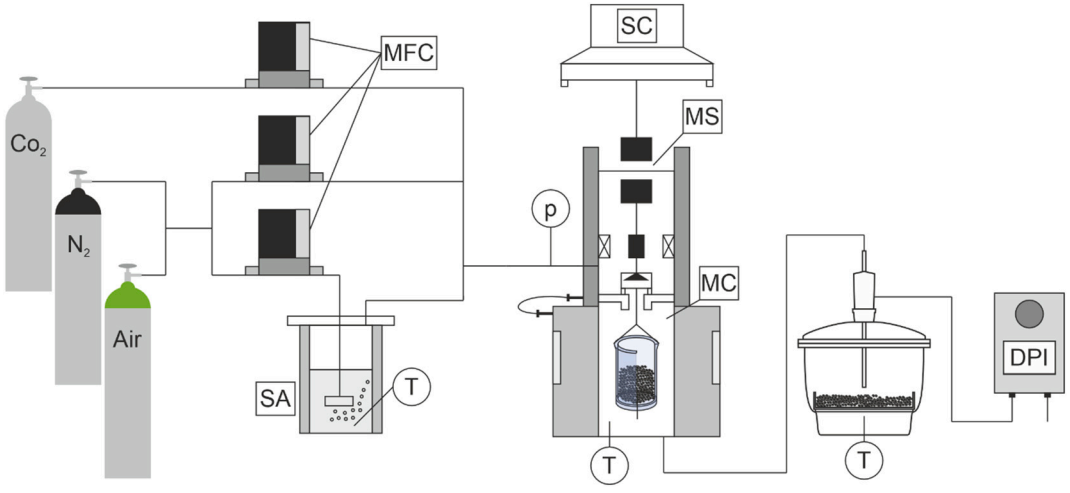

Fig. 1. Sorption apparatus in perfusion mode. The scale (SC) weighs the sample inside the closed and conditioned measurement cell (MC) via a magnetic suspension (MS). Additional material is exposed to the same gas stream in the desiccator. Pressure (p) and temperature (T) indicators monitor the process. The MC is perfused with gas from various dry-gas sources dosed via mass-flow controllers (MFC). The gas streams air and nitrogen are separated to saturate one stream with water. The settings of the MFC adjust the atmosphere in the MC and desiccator. The dew-point indicator (DPI) measures the water content of the gas stream.

min. Subsequently, the powder was added to the binder solution and mixed for 45 min at 2000 rpm in the disperser. With the addition of styrene-butadiene rubber (SBR BM-451-B, Zeon, Japan), the speed was reduced to 500 rpm and mixed for additional 20 min. Finally, degassing was performed in the rotary revolution mixer at 600 rpm and 250 mbar for 5 min. The slurry exhibited a solid content of 52 wt%.

For the cathode slurry preparation, environmental impacts were completely excluded by using an argon-filled ($c_{H2O} < 1$ ppm, $c_{O2} < 1$ ppm) glove box (GS MEGA *E*-LINE, GS Glovebox, Germany). Weighing and dosing of the slurry constituents were performed inside the inert gas environment, whereas for the mixing steps, the mixing container was transferred out of the glove box system in a sealed state and mixed within the rotary revolution mixer. The first step involved dry mixing a conductive additive (Super C65, Imerys, France) with polyvinylidene fluoride (PVDF Solef 5130, Solvay, Belgium) at 1000 rpm for 1 min. Next, *N*-methyl-2-pyrrolidone (NMP) (Merck, Germany) was added and mixed three times at 1600 rpm for 10 min with a 5 min break in between for cooling. Finally, NCM-622 (HED NCM-622, BASF, Germany) was introduced and mixed two times at 600 rpm for 10 min. The final solid content of the slurry was 55 wt%.

2.2. Coating, drying, calendering

The anode slurry was coated onto a 12 µm thick copper current collector (Schlenk, Germany) with a roll-to-roll coater (BC 50, Coatema, Germany) and doctor blade application using a web speed of 0.5 m min^{-1}. The three infrared dryers operated at temperatures of 45, 50, and 55 °C, resulting in an anode active material mass loading of 9.0 mg cm^{-2} (dry anode thickness of 70 µm). To reach the target porosity of 30%, calendering was performed on a calendering machine (EA 102, Coatema, Germany) with a maximum line load of 1000 N mm^{-1} and a roller diameter of 400 mm at a roller speed of 0.1 m min^{-1}.

The cathode was coated inside the glove box system on an aluminum current collector foil with a thickness of 15 µm (1100-L, Hydro, Norway) using an automated film coating device (AB3652, TQC Sheen, USA) with a doctor blade (ZUA 2000, Zehntner, Switzerland) at a coating speed of 50 mm s^{-1}. The cathode active material mass loading yielded 17.1 mg cm^{-2} (dry cathode thickness of 98 µm). The coated sheets were then vacuum-dried in the vacuum lock of the glove box system for 12 h at 70 °C with 20 vacuum and purging cycles between 120 and 570 mbar lasting 2 min each. Subsequently, the cathodes were compressed to the target porosity of 30% with a pressure of 3575 kg cm^{-2} and a holding period of 30 s via a uniaxial laboratory press (MP250, Maassen, Germany).

2.3. Cell assembly

The coin cells were assembled in the argon-filled glove box system. Before cell assembly, the components were vacuum-dried in the vacuum lock of the glove box system for 12 h at 90 °C and 120 mbar to reduce the residual moisture. All cells were composed of an anode (diameter of 15 mm, absolute capacity 5.67 mAh), a cathode (diameter of 14 mm, absolute capacity 4.47 mAh) (N/P ratio of 1.1), a 200 µm thick glass-fiber separator (diameter of 16 mm, Type 691, VWR, USA), two metal spacers (thickness of 1 and 0.5 mm), and a contact spring. As electrolyte, 100 µL of LP572 (BASF, Germany) containing 1 M lithium hexafluorophosphate ($LiPF_6$) conducting salt dissolved in a mixture of ethylene carbonate (EC) and ethyl methyl carbonate (EMC) in a mass ratio of 3:7 and 2 wt% vinylene carbonate was used and portioned onto the separator. For each test series, four coin cells were produced for a statistical evaluation.

2.4. Cell testing

To investigate the electrochemical behavior of the cells, formation and a rate capability test were conducted using a battery cycling system (CTS Lab, BaSyTec, Germany) and a climate chamber (ED-115, Binder, Germany) providing a constant temperature of 25 °C. The formation involved three charge-discharge cycles between the lower cutoff voltage of 2.9 V and the upper cutoff voltage of 4.2 V. For charging, a constant current (CC) of 0.1C was applied, whereby in the third cycle, a constant voltage (CV) phase at 4.2 V was added until a current below 0.02C was reached. Discharging was performed at a CC of 0.1C. The charging cycles in the rate capability test were carried out with a CC of 0.1C up to 4.2 V with an additional CV phase until the current fell below 0.02C. The discharge cycles comprised CC of 0.1C, 0.2C, 0.5C, 1C, 3C, and 5C, performing three cycles at each C-rate until the lower cutoff voltage of 2.9 V was reached. Subsequently, three check-up cycles were added, with CC charging and discharging at 0.1C and a CV charging phase at 4.2 V until the current dropped below 0.02C. The currents during formation were based on the theoretical capacities of the cells. For the C-rates in the rate capability test, the measured capacity of the third formation cycle was considered.

3. Results and discussion

3.1. Electrodes exposed to humid air (Long exposure)

In a long-term sorption experiment, displayed in Fig. 2, NMC-622 and NMC-811 cathodes (preparation cf. [22,29]) and graphite anodes were placed in humid air.

This experiment shows the different characteristics of the sorption behavior of graphite anodes and NMC cathodes in air. The y-axis plots the mass uptake in weight parts per million (wt-ppm) and the x-axis plots the uptake time in days. Each data point represents the average of three samples (two samples in case of the anodes) and their respective standard error. This sorption experiment took place at a relative humidity (RH) of 72% at room temperature (~ 22 °C), corresponding to a dew-point temperature (DPT) of 17 °C.

The sorption of components of the atmosphere in these electrodes occurs on different time scales. The anodes reach their sorption equilibrium after ~30 h and do not change their mass over the course of this experiment excluding slight fluctuations. This observation confirms

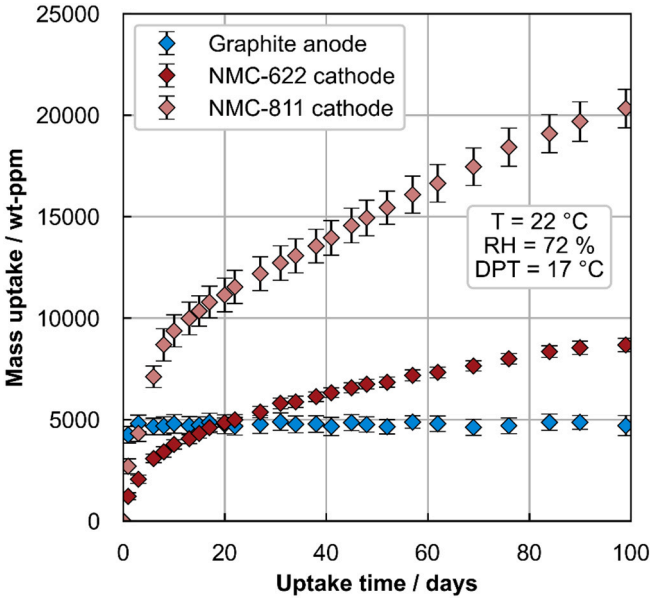

Fig. 2. Mass uptake over time of Li-ion battery electrodes in humid air (in a desiccator, setup 1) at room temperature. The mass uptake over time propagates differently for anode and cathodes. The anode quickly reaches equilibrium with the atmosphere, while the cathodes express (compared to the anode) a slow and steady mass uptake, with no equilibrium after 100 days of exposure. The chemistry of the NMC affects the mass uptake. The experiment indicates that the chemical reactions on the CAM limit the mass uptake.

previous studies, which showed that the components of graphite anodes physically ad- and absorb water [2,25,26]. These anodes serve as a control to ensure that the conditions in the desiccator are constant over time and the results of sorption experiments in the desiccator (setup 1) are plausible.

The cathode's sorption behavior in humid air differs from the anode's sorption behavior in humid air. The mass increase over time of the NMC cathodes is slower compared to the mass increase of the graphite anodes. Additionally, the rate of mass increase of the NMC-811 cathode is larger compared to the one of the NMC-622 cathode. Unlike the anodes, the cathodes do not reach an equilibrium state with the surrounding atmosphere in the considered time frame (up to 100 days). After 20 days the mass uptake of the cathodes transitions into an approximately linear mass uptake that slowly decreases over the course of the experiment.

Several kinetic factors could be responsible for the mass uptake of the cathodes. The mass transport of water and CO_2 from the bulk of the gas phase to the surface of the cathodes, the adsorption kinetics of these two molecules to the surface, and the reaction kinetics of the hydroxide and carbonate formation.

The electrode samples all have the same dimensions and rest in identical weighing glasses. If gas-phase mass transport of water to the electrode surfaces were the dominant kinetic process, the mass uptake of all three electrodes would either be identical or larger for the cathodes (because of the additional CO_2 uptake). The anode only absorbs water and initially has a larger mass-uptake rate than the cathodes, it can therefore be concluded that enough water for adsorption, absorption and chemisorption is present at the surface of the cathodes. This indicates that the water mass transport in the gas phase does not limit the mass uptake of the cathodes.

As the mass uptake rate of the cathodes depends on the chemistry of the active material, it appears that the reaction kinetics on the cathodes are responsible for the mass uptake over time. An overlap of these reaction kinetics and the mass transport of CO_2 to the surfaces of the cathodes is possible.

This experiment shows that the sorption of graphite anodes and NMC cathodes are different regarding time scales, equilibria, and kinetics. Chemical reactions appear to be a responsible kinetic factor for the mass uptake of NMC cathodes in humid air. The cathodes with a larger nickel content have a larger mass uptake.

3.2. *Effect of humid nitrogen vs. humid air*

Any following results were obtained with NMC-622 raw material to exclude influences of other components of an electrode (e.g., binder and current collector). A differentiation between the sorption of water and CO_2 in CAM and the sorption of just water in CAM is possible by changing the atmosphere. Chen et al. found that the chemical reaction of NMC-811 and CO_2 is triggered by the presence of water [30], similar mechanisms are expected for NMC-622. Using high resolution transmission electron microscopy (HRTEM), Zou et al. showed that NMC-811 is noble against CO_2, O_2, and N_2 [18]. Furthermore, they showed that the hydroxide formation in the presence of water on the surface of NMC-811 is self-passivating. Once this hydroxide layer is formed, the material is no longer noble against CO_2 and carbonate forms on its surface [18]. Fig. 3 shows mass uptake over time in humid atmospheres made of air and nitrogen measured in a magnetic sorption balance (setup 2).

The samples were exposed to nitrogen and air at a RH of 2.3% (DPT = −20 °C). During the sorption experiment in the nitrogen atmosphere the NMC-622 reaches equilibrium at ~60 wt-ppm. During the sorption experiment in the air the NMC-622 does not reach an equilibrium. The mass uptake continues for 100 h. O_2, CO_2 (and small quantities of noble gases) are present in the gas phase during the sorption experiment with NMC-622 in air in comparison to the sorption experiment with NMC-622 in nitrogen. Literature suggests that CO_2 makes the difference between these two experiments even at the low concentration of 400 vol-ppm in air. As the sorption occurring in humid air does not reach an equilibrium, there is no self-passivating effect.

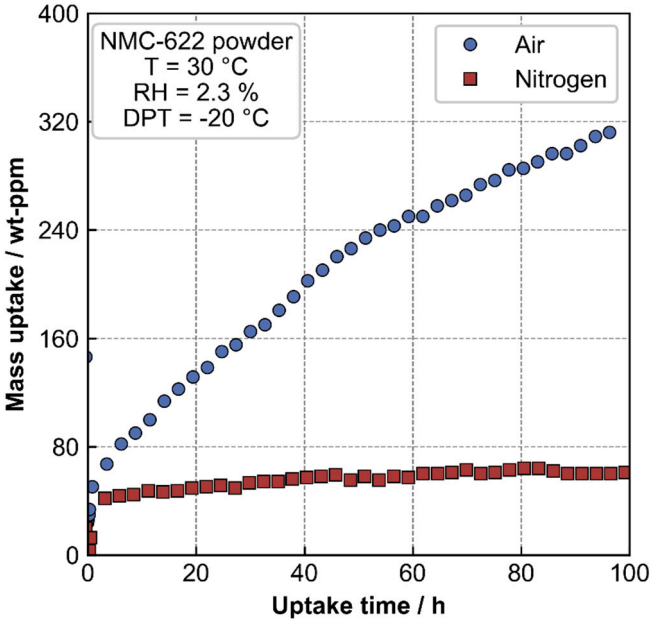

Fig. 3. Sorption behavior of NMC-622 in humid atmospheres (air and nitrogen). The relative humidity is 2.3% in both atmospheres at an air temperature of 30 °C. The mass uptake over time expresses a characteristic propagation for each atmosphere. The sorption with water in nitrogen reaches equilibrium. The sorption in humid air does not reach equilibrium. Red data points are reproduced with permission from [20] copyright [2024] American Chemical Society. (For interpretation of the references to colour in this figure legend, the reader is referred to the web version of this article.)

The initial mass uptake (3*h*) of the sorption experiment in air is similar to the sorption experiment in nitrogen. Both samples reach 50 ppm before the rate of the mass uptake changes. This shows that the sorption responsible for this mass uptake occurs in both atmospheres. After the initial uptake, the mass-uptake rate in humid nitrogen continues slowly, compared to the exposure to air, and reaches equilibrium. The mass uptake in air also slows down after the initial uptake but remains approximately constant over 100 h. This change indicates that kinetics associated with CO_2 on the surface of the NMC-622 restrict the mass uptake, as it is the only difference (apart from inert O_2 to the sorption in nitrogen).

Consequently, the species formed during sorption experiments in both atmospheres should differ. A desorption at two temperatures yields information about the species. Carbonates and hydroxides such as LiOH and Li_2CO_3 decay at temperatures above 500 °C [15]. Therefore, sorbate with weak bonds should be desorbed at 115 °C, while other species will remain intact. Fig. 4 plots the mass uptake as well as the residual mass uptake after exposing the sample at 30 °C (dark blue bar) and at 115 °C (light blue bar) to dry nitrogen.

The mass uptake is plotted in wt-ppm for experiments conducted in air (Fig. 4, left) and nitrogen (Fig. 4, right). Both atmospheres had a DPT = −20 °C (RH of 2.3%) during the sorption experiment. The determination of the residual mass uptake took place in dry nitrogen (DPT ~ −65 °C). The mass uptake in air is larger by a factor of five compared to nitrogen for the same sample geometry and exposure time.

35% of the mass attached to the NMC-622 during the sorption experiment in nitrogen desorbed at 30 °C (the temperature of the sorption experiment). The residual mass at 115 °C is about 10% of the initial mass uptake. This circumstance shows that the mass (in this case water) requires more energy than available at 30 °C to detach. However, most of the mass uptake is reversable at 115 °C, which is below the degradation temperature of species e.g., LiOH, cf. [29].

In contrast, the reversible part after the sorption experiment in air is

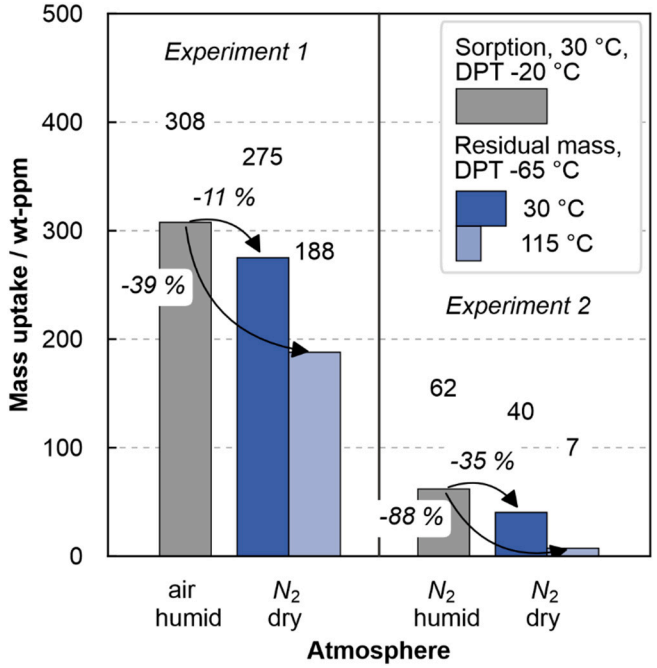

Fig. 4. Mass uptake of NMC-622 after sorption experiments and the residual mass uptake after exposure to dry nitrogen at 30 °C and at 115 °C. The mass uptake in air is larger compared to the one in nitrogen. The reversible mass uptake at 30 °C is proportionally larger in nitrogen compared to air as is the reversible mass uptake after exposure to dry nitrogen at 115 °C.

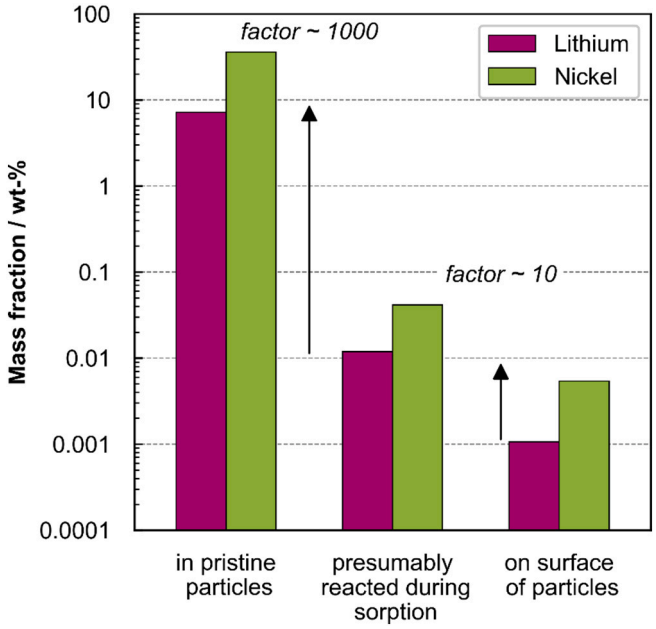

Fig. 5. Comparison of the chemical composition of the pristine particles to the presumably reacted amount of lithium and nickel and the number of atoms on the surface of the pristine particles in the CAM NMC-622. The calculation assumes that either lithium or nickel is responsible for the irreversible mass uptake from Fig. 4. Note the **logarithmic scale** of the y-axis. The calculation shows that only a small fraction of the initial lithium of the CAM is chemically bound, even less for nickel. However, the lithium/nickel-atoms on the surface of the particle do not suffice to explain the irreversible mass uptake. This suggests that the overall effect of this mass uptake is small. However, the surface of the material should be heavily altered.

smaller. 11% of the mass detached from the NMC-622 at 30 °C and 39% detached at 115 °C. Therefore, possible species that form are likely carbonates and hydroxides, with higher degradation temperatures than 115 °C. This circumstance confirms the conclusion from the kinetic observation from Fig. 3, that the mass uptake in air is a chemical reaction of CO_2 and water with NMC-622. Further characterization of the exposed raw material is possible via high-resolution transmission electron microscopy, scanning electron microscopy, X-ray diffraction, and X-ray photoelectron spectroscopy as shown in other studies [11,18,30–32]. The focus of this study is on the gravimetric analysis of the chemical sorption, therefore, in the following, the mass that remains attached to the raw material after exposure to 115 °C will be assessed via calculation.

3.3. Evaluation of the chemically bound mass

The assumption that the irreversible mass uptake after desorption at 115 °C is the product of the chemical reactions leads to the evaluation plotted in Fig. 5. This assessment puts the mass uptake from Fig. 4 into perspective. Results from literature propose several possible reactions. Sicklinger et al. found experimental evidence that the formation of basic nickel carbonate is plausible [15]. Other studies claim the reaction from lithium in the NMC-622 crystal to LiOH and Li_2CO_3 is the dominate reaction [14,33–35]. The calculations for lithium and nickel assume that all the mass uptake (cf. Fig. 4) is the product of either the lithium reaction equations or the nickel reaction equations.

Fig. 5 plots the calculated mass fractions of lithium and nickel on a logarithmic y-axis. The mass fraction of lithium and nickel in the pristine particles is supplied by the producer. The mass fraction of lithium and/or nickel possibly reacted during sorption is calculated based on the irreversible part of the previous sorption experiment (Fig. 4). The mass fraction of lithium and nickel on the surface of the particles is derived from the BET-surface of the particles supplied by the producer. Additionally, it is assumed that lithium/nickel occurs on the surface of the particles according to the chemical formula of NMC-622. In approximation, the atoms are spaced according to the a-lattice constant in a cubic crystal structure (2.8 Å [36], omitting the complex lattice structure and its expansion during charging). The c-lattice constant is the largest lattice constant. Therefore, this approximation overestimates the number of atoms on the surface. Note the great difference of the mass fractions, which is underrepresented by the logarithmic scale. Details of the calculation can be found in the supporting information.

The mass fraction of lithium and nickel is ~1000 times larger than the mass fractions of lithium and nickel that might have reacted during the exposure to humid air (DPT = −20 °C). This comparison indicates that most of the structure remains intact. Additionally, according to the producer, the impurities of LiOH and Li_2CO_3 of the pristine material are 0.3 and 0.2 wt-%, respectively. Therefore, the initial impurities are one order of magnitude larger than the amount of impurities added by the exposure, also indicating the minor degradation effect induced by this exposure.

However, if the atoms on the surface are compared to the fraction of the reacted atoms, the exposure appears more severe: ~ ten times the number of atoms on the surface react during exposure. Possible explanations are the relocation of lithium to the surface of the material if water is in the gas phase [18]. While the difference in exposure in atmospheres with and without CO_2 is clearly observed, the quantitative effect of the exposure on the overall mass content of the metals in the particle is small. However, the surface structure should be heavily altered, which aligns with various optical observations in literature [11,15,19,30].

3.4. CO_2-concentration variation in the gas phase

The following experiments are conducted to evaluate if controlling the CO_2 concentration in the production atmosphere mitigates the degradation of the CAM. The influence of exposing the CAM to defined

atmospheres that contain water and CO_2 on cell performance is assessed at industrial humidity conditions. Furthermore, the influence of the CO_2-concentration in the gas phase on the sorption kinetics is considered based on the experimental data displayed in Fig. 6.

The data show the mass uptake of NMC-622 active material within four days in wt-ppm. The mass uptake over time changes depending on the CO_2 concentration (200, 400, and 800 vol-ppm CO_2) in the humid atmosphere (DPT of −38 °C). The mass uptake occurs in two approx. linear rates: first the mass increases by 160 wt-ppm within 20 h, second the mass increases by another 80 wt-ppm within the next 80 h. The mass uptake of NMC-622 in the 800 vol-ppm CO_2 atmosphere is larger than the uptake in the 400 vol-ppm CO_2 atmosphere. After the decrease in uptake rate after 20 h, the mass of the samples exposed to 800 vol-ppm CO_2 increases faster. The acceleration must result from the doubling of CO_2 concentration in the gas atmosphere, because all other parameters remained constant.

The mass uptake in the 200 vol-ppm CO_2 atmosphere is insignificantly different compared to the 400 vol-ppm CO_2 atmosphere. The standard error increases with decreasing CO_2 concentration in the atmosphere. An explanation for this increase could be the decreasing precision of the mass-flow controller towards its lower adjustment limit. The comparison of the 200 vol-ppm and the 400 vol-ppm CO_2 atmosphere exposure does not allow any conclusions. However, it confirms the comparison of the mass uptakes in the 400 vol-ppm and 800 vol-ppm CO_2 atmospheres as a trend.

A simulation of the gas-phase mass transport of CO_2 to the surface of the active material shows that sufficient CO_2 molecules diffuse to the surface to load the sample with 1000 wt-ppm CO_2 (cf. supporting information). The sample's mass-uptake of water and CO_2 is 250 wt-ppm in total. This circumstance indicates that mass transport of CO_2 from the bulk of the gas phase to the surface of the NMC-622 is not limiting the mass uptake.

The concentration of water in the atmosphere at a DPT of −38 °C is 160 ppm, which is less than the CO_2 concentration. It must be discussed whether water limits the mass-uptake. Experimentally, if the water concentration of the gas phase was limiting the uptake rate, the mass-uptake in Fig. 6 would not be dependent on the CO_2 concentration in the gas phase. The formation of lithium hydroxide requires water. However, the reaction of lithium hydroxide to lithium carbonate releases water (cf. supporting information and e.g. [19]). If the released water was available for further hydroxide formation, the carbonate formation would be self-sustaining. This circumstance could explain the experimental observation.

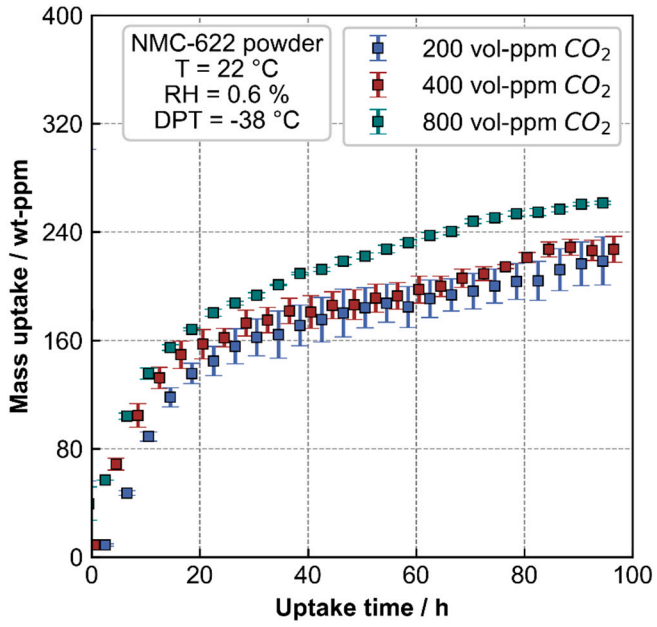

Fig. 6. Sorption behavior of NMC-622 active material in humidified nitrogen with additional CO_2. The mass uptake increases with increasing CO_2 concentration in humidified nitrogen. The mass uptake after ~4 days is below 400 wt-ppm for all CO_2 concentrations. Compared to the total mass uptake of the experiment, the mass-uptake increase due to the change of CO_2 concentration in the nitrogen is small.

In absolute terms, the mass uptake in any case is rather small over four days and a change in CO_2 concentration has a small effect on the mass uptake for the investigated atmospheres. However, these experiments also indicate that kinetics associated with the CO_2 concentration limit the mass uptake.

3.5. Electrochemical data

Along with the experiments from Fig. 6, additional CAM as raw material was exposed to the same atmosphere as the weighed sample (cf. Fig. 1). It is assumed that the additionally exposed NMC-622 experienced a similar amount of mass uptake as the weighed sample, as it was exposed to the same atmosphere at room temperature (DPT = -38 °C) for the same time. This additional CAM was processed in argon filled gloveboxes into electrodes and eventually coin cells, which were tested. The processing in gloveboxes after the defined exposure ensures that further chemical sorption is mitigated. The impact of the exposure on the electrochemical performance is shown in Fig. 7.

Plot a) shows the formation cycles of the coin cells produced with the exposed CAM compared to reference cells produced with pristine material that were not exposed. Cells with reference CAM and the CAM exposed to 200 vol-ppm and 400 vol-ppm CO_2 show similar specific discharge capacities. This is indicated by the 0.1C cycles with overlapping standard deviations. A significant difference was observed for the cells built from CAM exposed to 800 vol-ppm CO_2. The specific capacity is reduced by about 1.6%.

Plot b) shows an overall similar normalized C-rate performance for all cells with overlapping standard deviations. However, a low standard deviation for the cells containing CAM exposed to 800 vol-ppm CO_2 is noticeable. It shows that exposing CAM to an atmosphere with 800 vol-ppm CO_2 affects C-rate performance. The cells built with CAM exposed to 800 vol-ppm CO_2 perform worse than the reference in terms of rate capability. This difference decreases minimally at 5C compared to the 2C and 3C cycles. The charge-transfer resistance seems to be impacted by the CO_2 exposition at 800 vol-ppm CO_2 of the CAM. The data of the cells built with CAM exposed to 200 and 400 vol-ppm CO_2 confirm this trend.

Comparing the results of this study to similar studies is challenging because the exposure time, relative humidity, used active materials, and processing of the cells greatly vary. However, some studies allow a qualitative comparison. Chen et al. built NMC-622 half-cells with pristine material, and material stored in a humidity chamber at 55 °C and 80%-RH [17]. While the first cycles of their half-cells built with pristine CAM show a specific capacity like the full cells of this study, the half-cells built with stored CAM express a reduced specific capacity of $< -50\%$. This specific capacity reduction observed by Chen et al. is large compared to the specific capacity reduction observed in Fig. 7. This effect can be attributed to the different storage conditions. Fenske et al. exposed graphite anode, NMC-622 cathode, and separator to humified argon at DPT between 0 °C and - 60 °C during cell assembly [8]. They focused on the effect of water content of the components on the cell performance. The specific discharge capacity of cells assembled in an atmosphere with a DPT of - 30 °C and below observed by Fenske et al. ranges between 167 and 170 mAh/g_{CAM}. This specific discharge capacity is about 2% larger than the discharge capacity in this study. Comparing the effect of storage conditions from this study to the effect of the water content of the cell components is impossible. However, considering both results show that a production atmosphere with a DPT of - 40 °C has little effect on the cell performance, if the material is stored

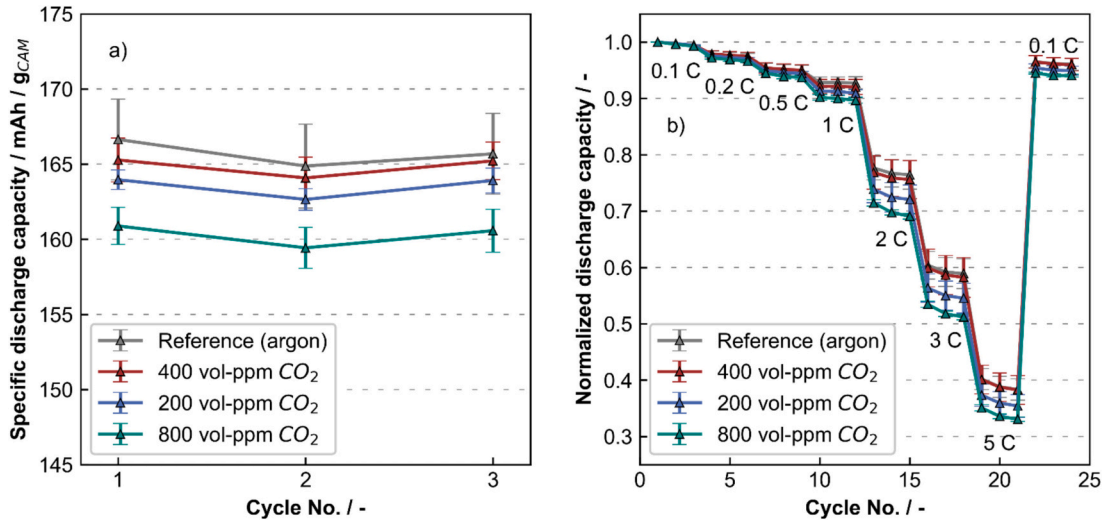

Fig. 7. Cell test results for full coin cells with differently CO_2-exposed CAM. Subplot a) shows the formation cycles at a C-rate of 0.1C and b) the normalized C-rate test cycles. The exposure of the cathode active material affects cell performance. The difference in the formation cycles of the unexposed reference and the material exposed to 400 vol-ppm, and 200 vol-ppm is not statistically significant. The 800 vol-ppm exposed material performs slightly worse during formation than the other samples. The results of the C-rate tests follow the trend of the results for the formation cycles.

or the cells are assembled in such conditions.

An unexpected observation is that the CAM exposed to 400 vol-ppm CO_2 performs slightly better than the CAM exposed to 200 vol-ppm CO_2. However, as observed in the sorption data, this difference is not statistically significant. The electrochemical results for the 800 vol-ppm CO_2 variant are in line with the detected mass uptake from Fig. 6. The reduction of the initial capacity could originate from carbonate formation, leading to the consumption of Li-ions. However, the overall difference is small, which indicates that the exposure in this study did not strongly deteriorate the CAM. This shows that the variation of the CO_2 concentration has only a little effect on the cell performance at a DPT of −38 °C. Unprotected NMC-CAM with a higher nickel content are expected to be more susceptible to degradation. Analyzing the electrolyte of the cells post mortem via nuclear magnetic resonance spectroscopy [37–39] could provide information on how the degraded CAM affects the decomposition reactions. However, such experiments are beyond the scope of this study and are suggested for future studies.

4. Conclusion

This study probed the sorption of water and CO_2 in NMC-622 and NMC-811 cathodes. Focusing on the cathode active material NMC-622, the sorption data shows time-resolved mass uptakes in various atmospheres. These atmospheres range from (DPT ~16 °C) to industrial atmospheres (DPT ~ -40 °C). The following conclusions regarding characteristics and kinetic limitations during the sorption of water and CO_2 in NMC-622 are possible.

The presence of CO_2 changes the sorption characteristics of NMC-622 in humid atmosphere. Sorption with water and CO_2 is not passivating, while sorption with water and without CO_2 is passivating at the considered DPT. The bond of the absorbed molecules is stronger if CO_2 is present in humid atmosphere compared to the sorption in a humid atmosphere without CO_2. An estimate suggests that the surface of the material should be heavily altered. However, the overall mass uptake of the CAM at conditions below a DPT of −20 °C is small after four days of exposure. The electrochemical evaluation of the CAM after 4 days of sorption at a DPT of −38 °C and 200, 400, and 800 vol-ppm CO_2 shows that the small mass uptake, compared to the entire mass of the CAM, has little but noticeable effect on the electrochemical performance of the material. However, comparing the cell data of the unexposed reference to the cell data of the CAM exposed to 800 vol-ppm CO_2 showed that the cells built with exposed material performed worse. This effect is attributed to a mass uptake of 250 wt-ppm.

Comparing the sorption kinetics of water and CO_2 in NMC-811 and NMC-622 cathodes shows that material chemistry affects the mass uptake rate. This indicates that material specific kinetics govern mass transport, as sorption conditions for both samples were similar. The variation of the CO_2 concentration during sorption suggests a kinetic limitation associated with CO_2 uptake. Carbonate formation, lithium leaching, or a combination are imaginable. The effect of a variation of the water concentration on the mass uptake was not specifically addressed here and should be investigated as well.

CRediT authorship contribution statement

Thilo Heckmann: Writing – review & editing, Writing – original draft, Visualization, Project administration, Methodology, Investigation, Formal analysis, Data curation, Conceptualization. **Maximilian Lechner:** Writing – review & editing, Writing – original draft, Methodology, Investigation, Formal analysis, Data curation, Conceptualization. **Philipp Barbig:** Writing – review & editing, Methodology, Investigation, Data curation, Conceptualization. **Xiangling Gui:** Investigation, Formal analysis, Data curation. **Lukas Madlindl:** Methodology, Investigation, Data curation, Conceptualization. **Philip Scharfer:** Writing – review & editing, Supervision, Resources, Project administration, Methodology, Funding acquisition. **Rüdiger Daub:** Writing – review & editing, Supervision, Resources, Project administration, Funding acquisition. **Wilhelm Schabel:** Writing – review & editing, Supervision, Resources, Project administration, Funding acquisition.

Declaration of competing interest

The authors declare that they have no known competing financial interests or personal relationships that could have appeared to influence the work reported in this paper.

Acknowledgments

The authors gratefully thank the German Federal Ministry of Education and Research (BMBF) for the financial support via InMiTro (03XP0345A and 03XP0345C) and Epic (03XP0295A) within the InZePro and ProZell competence clusters. The authors also thank Jochen C.

Eser, Aliénor Potthoff, Josef Keilhofer, Fabienne Huttner, and Carina Heck, for experimental support and fruitful discussions.

Appendix A. Supplementary data

Supplementary data to this article can be found online at https://doi.org/10.1016/j.est.2026.120994.

Data availability

Data will be made available on request.

References

[1] A. Kwade, W. Haselrieder, R. Leithoff, A. Modlinger, F. Dietrich, K. Droeder, Current status and challenges for automotive battery production technologies, Nat. Energy 3 (2018) 290–300, https://doi.org/10.1038/s41560-018-0130-3.
[2] J.C. Eser, B. Deichmann, T. Wirsching, P.G. Weidler, P. Scharfer, W. Schabel, Hysteresis behavior in the sorption equilibrium of water in anodes for Li-ion batteries, Langmuir ACS J. Surf. Colloids 36 (2020) 6193–6201, https://doi.org/10.1021/acs.langmuir.0c00704.
[3] S.N. Bryntesen, A.H. Strømman, I. Tolstorebrov, P.R. Shearing, J.J. Lamb, O. Stokke Burheim, Opportunities for the state-of-the-art production of LIB electrodes—A review, Energies 14 (2021) 1406, https://doi.org/10.3390/en14051406.
[4] J. Kaiser, V. Wenzel, H. Nirschl, B. Bitsch, N. Willenbacher, M. Baunach, M. Schmitt, S. Jaiser, P. Scharfer, W. Schabel, Prozess- und Produktentwicklung von Elektroden für Li-Ionen-Zellen, Chem. Ing. Tech. 86 (2014) 695–706, https://doi.org/10.1002/cite.201300085.
[5] M. Armand, P. Axmann, D. Bresser, M. Copley, K. Edström, C. Ekberg, D. Guyomard, B. Lestriez, P. Novák, M. Petranikova, W. Porcher, S. Trabesinger, M. Wohlfahrt-Mehrens, H. Zhang, Lithium-ion batteries – Current state of the art and anticipated developments, J. Power Sources 479 (2020) 228708, https://doi.org/10.1016/j.jpowsour.2020.228708.
[6] M. Lechner, A. Kollenda, K. Bendzuck, J.K. Burmeister, K. Mahin, J. Keilhofer, L. Kemmer, M.J. Blaschke, G. Friedl, R. Daub, A. Kwade, Cost modeling for the GWh-scale production of modern lithium-ion battery cells, Commun. Eng. 3 (2024) 155, https://doi.org/10.1038/s44172-024-00306-0.
[7] H. Fenske, T. Heckmann, P. Michalowski, P. Scharfer, W. Schabel, A. Kwade, Impact of humidity on moisture resorption and resulting electrochemical performance of Gr/NMC622-based Li-ion batteries, J. Energy Storage 119 (2025) 116238, https://doi.org/10.1016/j.est.2025.116238.
[8] H. Fenske, T. Lombardo, J. Gerstenberg, C. Kern, D. Steckermeier, P. Michalowski, J. Janek, A. Kwade, Influence of moisture on the electrochemical performance of prelithiated graphite/SiO $_x$ composite anodes for Li-ion batteries, J. Electrochem. Soc. (2024), https://doi.org/10.1149/1945-7111/ad3856.
[9] F. Huttner, W. Haselrieder, A. Kwade, The Influence of Different Post-Drying Procedures on Remaining Water Content and Physical and Electrochemical Properties of Lithium-Ion Batteries, Energy Technol. 8 (2020) 1900245, https://doi.org/10.1002/ente.201900245.
[10] U. Langklotz, M. Schneider, A. Michaelis, Water Uptake of Tape-Cast Cathodes for Lithium Ion Batteries, J. Ceram. Sci. Technol. 4 (2013) 69–76, https://doi.org/10.4416/JCST2012-00036.
[11] M. Lechner, S. Wölfl, E. Kurz, R. Daub, Identification of critical moisture exposure for nickel-rich cathode active materials in lithium-ion battery production, J. Power Sources 626 (2025) 235661, https://doi.org/10.1016/j.jpowsour.2024.235661.
[12] N.V. Faenza, L. Bruce, Z.W. Lebens-Higgins, I. Plitz, N. Pereira, L.F.J. Piper, G. G. Amatucci, Editors' Choice—Growth of Ambient Induced Surface Impurity Species on Layered Positive Electrode Materials and Impact on Electrochemical Performance, J. Electrochem. Soc. 164 (2017) A3727–A3741, https://doi.org/10.1149/2.0921714jes.
[13] F. Degen, M. Winter, D. Bendig, J. Tübke, Energy consumption of current and future production of lithium-ion and post lithium-ion battery cells, Nat. Energy 8 (2023) 1284–1295, https://doi.org/10.1038/s41560-023-01355-z.
[14] A.R. Schuer, M. Kuenzel, S. Yang, M. Kosfeld, F. Mueller, S. Passerini, D. Bresser, Diagnosis tools for humidity-born surface contaminants on Li[Ni0.8Mn0.1Co0.1] O2 cathode materials for lithium batteries, J. Power Sources 525 (2022) 231111, https://doi.org/10.1016/j.jpowsour.2022.231111.
[15] J. Sicklinger, M. Metzger, H. Beyer, D. Pritzl, H.A. Gasteiger, Ambient Storage Derived Surface Contamination of NCM811 and NCM111: Performance Implications and Mitigation Strategies, J. Electrochem. Soc. 166 (2019) 2322–2335, https://doi.org/10.1149/2.0011912jes.
[16] R. Jung, R. Morasch, P. Karayaylali, K. Phillips, F. Maglia, C. Stinner, Y. Shao-Horn, H.A. Gasteiger, Effect of Ambient Storage on the Degradation of Ni-Rich Positive Electrode Materials (NMC811) for Li-Ion Batteries, J. Electrochem. Soc. 165 (2018) 132–141, https://doi.org/10.1149/2.0401802jes.
[17] Z. Chen, J. Wang, J. Huang, T. Fu, G. Sun, S. Lai, R. Zhou, K. Li, J. Zhao, The high-temperature and high-humidity storage behaviors and electrochemical degradation mechanism of LiNi0.6Co0.2Mn0.2O2 cathode material for lithium ion batteries, J. Power Sources 363 (2017) 168–176, https://doi.org/10.1016/j.jpowsour.2017.07.087.
[18] L. Zou, Y. He, Z. Liu, H. Jia, J. Zhu, J. Zheng, G. Wang, X. Li, J. Xiao, J. Liu, J.-G. Zhang, G. Chen, C. Wang, Unlocking the passivation nature of the cathode–air interfacial reactions in lithium ion batteries, Nat. Commun. 11 (2020) 3204, https://doi.org/10.1038/s41467-020-17050-6.
[19] I.A. Shkrob, J.A. Gilbert, P.J. Phillips, R. Klie, R.T. Haasch, J. Bareño, D. P. Abraham, Chemical Weathering of Layered Ni-Rich Oxide Electrode Materials: Evidence for Cation Exchange, J. Electrochem. Soc. 164 (2017) 1489–1498, https://doi.org/10.1149/2.0861707jes.
[20] T. Heckmann, L. Madlindl, P. Scharfer, W. Schabel, Increased Water Uptake of Li [Ni $_{0.6}$ Co $_{0.2}$ Mn $_{0.2}$]O $_2$ for Lithium-Ion Batteries in Humid Nitrogen above a Critical Gas Dew Point, ACS Appl. Energy Mater. 7 (2024) 1882–1889, https://doi.org/10.1021/acsaem.3c02976.
[21] F. Huttner, A. Marth, J.C. Eser, T. Heckmann, J. Mohacsi, J.K. Mayer, P. Scharfer, W. Schabel, A. Kwade, Design of Vacuum Post-Drying Procedures for Electrodes of Lithium-Ion Batteries, Batteries Supercaps 4 (2021) 1499–1515, https://doi.org/10.1002/batt.202100088.
[22] C.A. Heck, F. Huttner, J.K. Mayer, O. Fromm, M. Börner, T. Heckmann, P. Scharfer, W. Schabel, M. Winter, A. Kwade, Production of Nickel-Rich Cathodes for Lithium-Ion Batteries from Lab to Pilot Scale under Investigation of the Process Atmosphere, Energy Technol. 11 (2023) 2200945, https://doi.org/10.1002/ente.202200945.
[23] J. Kumberg, M. Müller, R. Diehm, S. Spiegel, C. Wachsmann, W. Bauer, P. Scharfer, W. Schabel, Drying of lithium-ion battery anodes for use in high-energy cells: Influence of electrode thickness on drying time, adhesion, and crack formation, Energy Technol. 7 (2019) 1900722, https://doi.org/10.1002/ente.201900722.
[24] W. Schabel, P. Scharfer, M. Kind, I. Mamaliga, Sorption and diffusion measurements in ternary polymer–solvent–solvent systems by means of a magnetic suspension balance—Experimental methods and correlations with a modified Flory–Huggins and free-volume theory, Chem. Eng. Sci. 62 (2007) 2254–2266, https://doi.org/10.1016/j.ces.2006.12.062.
[25] J.C. Eser, T. Wirsching, P.G. Weidler, A. Altvater, T. Börnhorst, J. Kumberg, G. Schöne, M. Müller, P. Scharfer, W. Schabel, Moisture Adsorption Behavior in Anodes for Li-Ion Batteries, Energy Technol. 8 (2020) 1801162, https://doi.org/10.1002/ente.201801162.
[26] J.C. Eser, B. Deichmann, T. Wirsching, L. Merklein, M. Müller, P. Scharfer, W. Schabel, Diffusion kinetics of water in graphite anodes for Li-ion batteries, Dry. Technol. 40 (2020) 1130–1145, https://doi.org/10.1080/07373937.2020.1852568.
[27] T. Heckmann, J.C. Eser, A. Altvater, J. Dörr, H. Lepère, P. Scharfer, W. Schabel, Mass transport in the Stefan-Knudsen transition region during vacuum drying at different pressures in a porous structure resembling battery electrodes, Langmuir ACS J. Surf. Colloids (2023), https://doi.org/10.1021/acs.langmuir.2c03450.
[28] F. Thurner, M. Stietz, Bestimmung der sorptionsisothermen lösungsmittelfeuchter sorbentien nach der durchströmungsmethode, Chem. Eng. Process. Process Intensif. 18 (1984) 333–340, https://doi.org/10.1016/0255-2701(84)87010-5.
[29] F. Huttner, A. Diener, T. Heckmann, J.C. Eser, T. Abali, J.K. Mayer, P. Scharfer, W. Schabel, A. Kwade, Increased Moisture Uptake of NCM622 Cathodes after Calendering due to Particle Breakage, J. Electrochem. Soc. 168 (2021) 090539, https://doi.org/10.1149/1945-7111/ac24bb.
[30] H. Chen, T. Ericson, R.H. Temperton, I. Källquist, H. Liu, C.N. Eads, A. Mikheenkova, M. Andersson, E. Kokkonen, W.R. Brant, M. Hahlin, Investigating surface reactivity of a Ni-rich cathode material toward CO_2, H_2O, and O_2 using ambient pressure X-ray photoelectron spectroscopy, ACS Appl. Energy Mater. 6 (2023) 11458–11467, https://doi.org/10.1021/acsaem.3c01621.
[31] Y. Ahn, Y.N. Jo, W. Cho, J.-S. Yu, K.J. Kim, Mechanism of Capacity Fading in the LiNi0.8Co0.1Mn0.1O2 Cathode Material for Lithium-Ion Batteries, Energies 12 (2019) 1638, https://doi.org/10.3390/en12091638.
[32] L. Yang, M. Takahashi, B. Wang, A study on capacity fading of lithium-ion battery with manganese spinel positive electrode during cycling, Electrochim. Acta 51 (2006) 3228–3234, https://doi.org/10.1016/j.electacta.2005.09.014.
[33] L. Britala, M. Marinaro, G. Kucinskis, A review of the degradation mechanisms of NCM cathodes and corresponding mitigation strategies, J. Energy Storage 73 (2023) 108875, https://doi.org/10.1016/j.est.2023.108875.
[34] G.V. Zhuang, G. Chen, J. Shim, X. Song, P.N. Ross, T.J. Richardson, Li2CO3 in LiNi0.8Co0.15Al0.05O2 cathodes and its effects on capacity and power, J. Power Sources 134 (2004) 293–297, https://doi.org/10.1016/j.jpowsour.2004.02.030.
[35] S.E. Renfrew, L.A. Kaufman, B.D. McCloskey, Altering Surface Contaminants and Defects Influences the First-Cycle Outgassing and Irreversible Transformations of LiNi0.6Mn0.2Co0.2O2, ACS Appl. Mater. Interfaces 11 (2019) 34913–34921, https://doi.org/10.1021/acsami.9b09992.
[36] R. Jung, F. Linsenmann, R. Thomas, J. Wandt, S. Solchenbach, F. Maglia, C. Stinner, M. Tromp, H.A. Gasteiger, Nickel, Manganese, and Cobalt Dissolution from Ni-Rich NMC and Their Effects on NMC622-Graphite Cells, J. Electrochem. Soc. 166 (2019) A378–A389, https://doi.org/10.1149/2.1151902jes.
[37] J.P. Allen, C.P. Grey, Solution NMR of Battery Electrolytes: Assessing and Mitigating Spectral Broadening Caused by Transition Metal Dissolution, J. Phys. Chem. C 127 (2023) 4425–4438, https://doi.org/10.1021/acs.jpcc.2c08274.
[38] S. Azam, W. Black, H. MacLennan, A. Adamson, E. Zsoldos, E.R. Logan, J.R. Dahn, Improving and Understanding Lifetime of LFP/Graphite Pouch Cells with Higher Concentrations of Vinylene Carbonate in the Electrolyte, J. Electrochem. Soc. 172 (2025) 070523, https://doi.org/10.1149/1945-7111/adf09c.
[39] R. Gauthier, H. Lin, V. Viswanathan, J. Whitacre, Nuclear magnetic resonance spectroscopy and differential capacity analysis as tools to study electrolyte consumption during the formation cycle of Li-ion pouch cells, J. Power Sources 657 (2025) 238134, https://doi.org/10.1016/j.jpowsour.2025.238134.